

A LACK OF RADIO EMISSION FROM NEUTRON STAR LOW MASS X-RAY BINARIES

MICHAEL P. MUNO,^{1,2} TOMASO BELLONI,³ VIVEK DHAWAN,⁴ EDWARD H. MORGAN,⁵ RONALD A. REMILLARD,⁵ AND
MICHAEL P. RUPEN⁴

Draft version November 11, 2018

ABSTRACT

We report strict upper limits to the radio luminosities of three neutron star low-mass X-ray binaries obtained with the Very Large Array while they were in hard X-ray states as observed with the *Rossi X-ray Timing Explorer*: 1E 1724–307, 4U 1812–12, and SLX 1735–269. We compare these upper limits to the radio luminosities of several black hole binaries in very similar hard states, and find that the neutron star systems are as faint as or fainter than all of the black hole candidates. The differences in luminosities can partly be attributed to the lower masses of the neutron star systems, which on theoretical and observational grounds are expected to decrease the radio luminosities as $M^{0.8}$. However, there still remains a factor of 30 scatter in the radio luminosities of black hole and neutron star X-ray binaries, particularly at X-ray luminosities of a few percent Eddington. We find no obvious differences in the X-ray timing and spectral properties that can be correlated with the radio luminosity. We discuss the implications of these results on current models for the relationship between accretion and jets.

Subject headings: X-rays: binaries — X-rays: individual: 1E 1724–307, 4U 1812–12, SLX 1735–269
— accretion — jets

1. INTRODUCTION

Astrophysical jets are observed from a wide range of systems, including active galactic nuclei (Lynden-Bell 1996), young stellar objects (Bachiller 1996), accreting white dwarfs in symbiotic binaries (Crocker et al. 2003; Sokoloski & Kenyon 2003) and super-soft X-ray sources (Cowley et al. 1998), and neutron stars and black holes in X-ray binaries (Fender 2004). Although it is generally accepted that the power supplied from these jets has its origin in accretion, the details of the mechanisms producing the jets are not fully established (e.g., Blandford & Payne 1982; Meier et al. 2001; Heinz & Sunyaev 2003, Falcke, Körding, & Markoff 2004). Observationally, one possible impediment to understanding these mechanisms is that the jets probably form on the time scales at which changes occur in the accretion flow (e.g., the viscous time scale; see Hartmann & Kenyon 1996; Mirabel et al. 1998; Sokoloski & Kenyon 2003). For young stellar objects and active galactic nuclei, that time scale is months to years, which makes it difficult to obtain well-sampled observations of jets as they form. Therefore, in trying to establish what conditions are needed to produce jets, it is often hard to disentangle the relative importance of the state of the accretion flow from the physical properties of the systems as a whole, such as the binary orbital period or the rotation rate of the accreting object. The exceptions are accreting compact objects, in which, because of their small size, the structure of their accretion flows are observed to change on time scales of hours to days.

Recent observations of X-ray binaries have provided the first information about the time-dependent relationship between the accretion flow and the formation of jets (e.g., Mirabel et al. 1998; Fomalont, Geldzahler, & Bradshaw 2001; Fender et al. 2004; Fender, Gallo, & Belloni 2004).

A particularly striking picture of the relationship between accretion and jets has emerged for black hole X-ray binaries (see Fender 2004, for a review). The accretion flows can be characterized by three “states” based on the spectral and timing properties of their X-ray and gamma-ray emission (0.5–500 keV): (1) a hard state that usually occurs at relatively low accretion rates in which the X-ray emission forms a power-law with photon index $\Gamma \approx 1.5 - 2.0$ that is exponentially cutoff at an energy of ~ 100 keV, and the power spectrum resembles band-limited white noise with a power of 10–30% rms, (2) a thermal state at higher accretion rates, in which the X-ray emission resembles that expected from a canonical optically-thick, geometrically-thin accretion disk with a temperature of ~ 1 keV (Shakura & Sunyaev 1973), and in which the power spectrum exhibits only weak noise (1–6% rms) with a power-law shape; and (3) a steep power-law state that is characterized by the sum of thermal emission plus a power-law of photon index $\Gamma = 2 - 3$ that extends without a break to ~ 500 keV, and the power spectrum usually contains quasi-periodic oscillations at low-frequency (0.1–20 Hz), and less often at high frequencies (150–450 Hz) or in the mHz range (see McClintock & Remillard 2004, for further discussion).

The radio emission associated with these states comes in two forms. First, optically thick radio emission from compact jets that extend only tens of AU (Dhawan, Mirabel, & Rodríguez 2000; Stirling et al. 2001) is observed to coincide with the X-ray hard power-law state ($\Gamma = 1.5 - 2.0$; Brocksopp et al. 1999; Corbel et al. 2000, Gallo, Fender, & Pooley 2003). The hard states and their jets can persist for days to months with relatively steady flux, and yet the jets become quenched

¹ Department of Physics and Astronomy, University of California, Los Angeles, CA 90095; mmuno@astro.ucla.edu

² Hubble Fellow

³ INAF — Osservatorio Astronomico di Brera, Via E. Bianchi 46, I-23807, Merate, Italy

⁴ National Radio Astronomy Observatory, Socorro, NM 87801

⁵ Center for Space Research, Massachusetts Institute of Technology, Cambridge, MA 02139

when sources enter thermal-dominated states.⁶ Second, transitions between these states are often observed to coincide with the formation of discrete synchrotron-emitting structures that travel relativistically across the sky (e.g., Mirabel & Rodríguez 1994; Fender et al. 1999; Fomalont et al. 2001; Fender & Kuulkers 2001). These ballistic jets form on time scales of a day, and eventually travel thousands of AU from the central black hole.

X-ray binaries containing neutron stars with relatively weak magnetic fields ($B \lesssim 10^9$ Gauss; these are almost always found in low-mass X-ray binaries, or LMXBs) resemble black hole systems in some respects, because the inner edge of the accretion disk can extend to near the inner most stable General Relativistic orbit in both types of systems. However, the relationship between X-ray and radio emission from neutron star LMXBs has not been as firmly established. Similarly to the black hole X-ray binaries, neutron star LMXBs exhibit a hard X-ray state with a $\Gamma \approx 1.5 - 2.0$. However, the analogs of the thermal-dominated and steep power-law states appear to be replaced by soft states in which most of the X-ray emission is produced by the boundary between the accretion disk and the neutron star (e.g., van der Klis 1995; Done & Gierliński 2003). Transient radio emission has been observed from neutron star X-ray binaries during periods in which their X-ray spectrum was highly variable (Penninx et al. 1988; Berendsen et al. 2000; Homan et al. 2003; Migliari et al. 2003, e.g.), and in two cases this emission was resolved into ballistic jets (Fomalont et al. 2001; Fender et al. 2004a). However, the peak luminosity of their radio emission is a factor of ≈ 30 lower than the black hole systems Fender & Kuulkers (2001). Two neutron star systems were also detected in persistently soft states (4U 1820–30 and Ser X-1; Migliari et al. 2004); this emission does not easily fit into the paradigm derived from black holes. However, no study has systematically targeted neutron star X-ray binaries in their hard, $\Gamma = 1.5 - 2.0$ power-law states to determine whether or not they exhibit steady, compact radio jets.

In this paper, we search for radio emission from three neutron star LMXBs in hard X-ray states with the Very Large Array (VLA) in order to determine whether the formation of compact jets affected by changing the central compact object from a black hole to a neutron star. We have observed three systems that remained in hard, $\Gamma = 1.5 - 2.0$ power-law states for the first five years of observations with the *Rossi X-ray Timing Explorer (RXTE)*: 1E 1724–307 in Terzan 2, SLX 1735–269, and 4U 1812–12. Each of these systems exhibits thermonuclear X-ray bursts, which demonstrates unambiguously that they contain neutron stars (Grindlay et al. 1980; Murakami et al. 1983; Bazzano et al. 1997). However, their X-ray properties are otherwise almost indistinguishable from those of black holes in their hard states (Olive et al. 1998; Wijnands & van der Klis 1999; Barret et al. 1999, 2000; Belloni, Psaltis, & van der Klis 2002; Barret et al. 2003).

The organization of this paper is as follows. In Section 2.1, we explain how we selected our sample of

sources, and report on the X-ray emission derived with *RXTE*. We include considerable detail in order to establish the degree to which these systems resemble black hole X-ray binaries in the hard state. In Section 2.2, we report on strict upper limits to the radio emission from three LMXBs in our sample that were obtained with the VLA, nearly simultaneous with the *RXTE* observations. In Section 3, we discuss the implications of a lack of radio emission from neutron star LMXBs in the hard state.

2. OBSERVATIONS

The basic observational properties of the three neutron star LMXBs that we have studied are listed in Tables 1 and 2.

2.1. *RXTE*

RXTE carries three instruments: the All-Sky Monitor (ASM), consisting of three, 30 cm² proportional counters sensitive between 1.5–12 keV that scan 80% of the sky every 90 minutes (Levine et al. 1996); the Proportional Counter Array (PCA), consisting of five, 1300 cm² detectors that record events with capability for microsecond time resolution and 256 channels of spectral resolution between 2–60 keV (Jahoda et al. 1996); and the High Energy X-ray Timing Experiment, consisting of two clusters of scintillation detectors, each with an effective area of 800 cm² and sensitivity between 15–250 keV (HEXTE; Rothschild et al. 1998). Data from all three instruments was used to characterize the X-ray emission from the LMXBs in our sample.

We first used data from the PCA and ASM to identify several neutron star LMXBs that persistently remained in a hard state (sometimes also referred to as the “island” of the atoll-shape in the color-color diagram) from the sample of systems that exhibit thermonuclear X-ray bursts (D. Galloway et al., in preparation). We first confirmed that the X-ray emission was steady using data from the *RXTE* ASM. We then measured the hardness of the X-ray spectrum using a hard color, which was defined as the ratio of the background-subtracted PCA counts in the (8.6–18.0)/(5.0–8.6) keV energy bands, where the counts were normalized to account for changes in the gain of the proportional counter units (see Muno, Remillard, & Chakrabarty 2003). Eight sources qualified as persistently hard, and we were able to obtain *RXTE* and VLA observations with a day of each other for three of these sources: 4U 1812–12, SLX 1735–269, and 1E 1724–307.⁷ The ASM light curves and PCA color-color diagrams from 8 years of observations are displayed in Figure 1. In the remainder of this section, we report the X-ray spectral and timing properties from *RXTE* observations taken within 6 weeks of the VLA observations.

2.1.1. *X-ray Spectra*

To produce spectra, we extracted data in 128 energy channels from the top layer of each active detector of the PCA, and in 64 channels from cluster 0 of HEXTE. For the PCA, the detector response and background were estimated using standard tools in FTOOLS version 5.1.

⁶ Note that it is unclear whether optically thick radio emission accompanies the rarer steep power-law states (e.g., Tavani et al. 1996; Fender et al. 2004b).

⁷ The sample of persistently hard neutron star LMXBs also includes 4U 1323–619, SAX J1712.6–3739, GS 1826–25, 4U 1832–330, and 4U 1850–087.

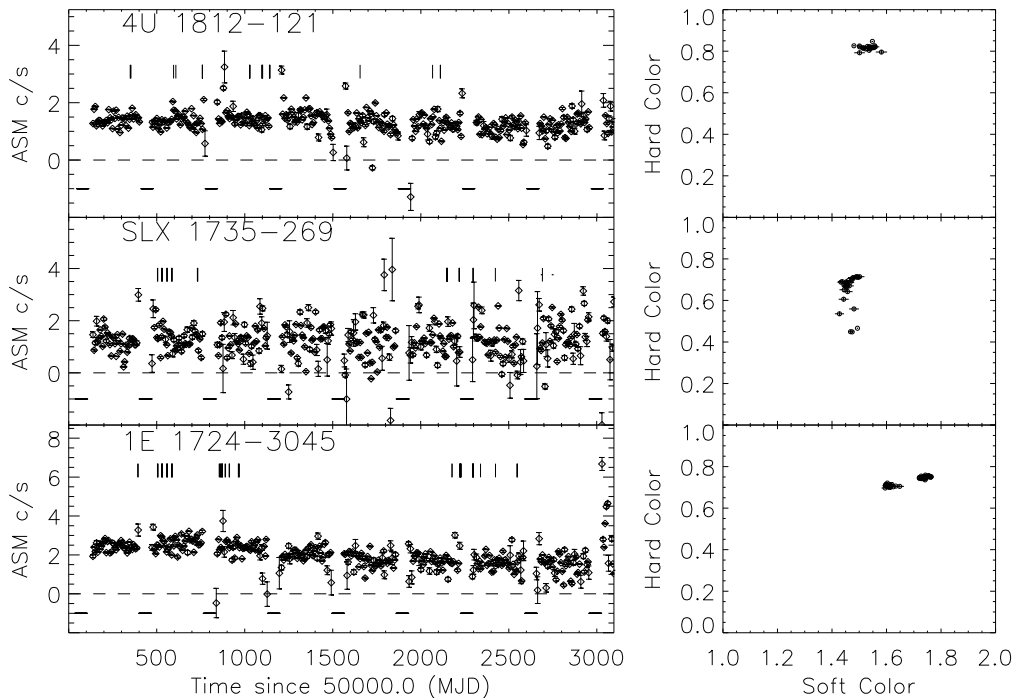


FIG. 1.— ASM light curves and PCA color-color diagrams illustrating the stability of the X-ray emission from the three sources we studied. The *left panels* plot weekly averages of the individual 90 s dwells. The horizontal bars at a count rate of -1 indicate periods when the sun was within 35° of the source. The vertical bars indicate the times of PCA observations, a subset of which were analyzed in detail for this paper. The *right panels* contain the hard and soft colors from the PCA data, which are defined as the ratio of the background-subtracted detector counts in the $(3.6-5.0)/(2.2-3.6)$ keV and the $(8.6-18.0)/(5.0-8.6)$ keV energy bands, respectively. All of the sources remained in the hard portion of the color-color diagram prior to 2001, although SLX 1735-269 became softer during observations in 2002 January.

For HEXTE, the background from the intervals in which the cluster was pointed off-source, and the response and effective area estimates were obtained from CALDB version 2.23. We modeled the spectra jointly in XSPEC version 11.2, using the 3–25 keV energy range from the PCA, and the 15–200 keV energy range from HEXTE. We applied a constant normalization to account for differences in the calibrated effective area of the PCA and HEXTE, and a 1% systematic uncertainty added in quadrature to the count spectra from the PCA to account for uncertainties in the detector calibration near the Xe edge at 4.5 keV. After confirming that the spectrum did not vary significantly over the course of the observations that we considered, we averaged the spectra to obtain better signal-to-noise at high energies. The resulting spectra are displayed in Figure 2.

We modeled the spectra using a phenomenological model that included a power-law continuum that produced most of the 2.5–200 keV flux; a blackbody component at low energies to remove residuals below 4 keV, which could result from emission from the neutron star’s surface or the inner accretion disk; a reflection component to account for residuals between 6–7 and 10–20 keV (refsch in XSPEC Fabian et al. 1989; Magdziarz & Zdziarski 1995), which may be produced by hard X-rays impinging on an optically thick accretion disk; and low-energy absorption caused by interstellar gas. The column density of interstellar matter (N_{H}) was fixed to the values determined from previous ob-

servations of each source by either *ASCA* or *BeppoSAX* (David et al. 1997; Guainazzi et al. 1998; Barret et al. 1999, 2003). The parameters of the reflection component could not all be constrained independently, so we fixed the inner and outer radii of the disk to 10 and 100 gravitational radii (GM/c^2), the power law index for reflection emissivity to -2 , the metal abundances to their solar values, the inclination to 30° , the disk temperature to 30,000 K, and the ionization fraction to 100. The final model is listed in Table 3. The black body and reflection components were only needed to obtain an acceptable χ^2/ν for SLX 1735-269 and 4U 1812-12, and so were not included in the model of 1E 1724-307.

The spectra of these neutron star LMXBs are qualitatively similar to those of black hole candidates in their hard states, such as Cyg X-1 (Di Salvo et al. 2001, e.g.) and GX 339-4 (Wilms et al. 1999, e.g.). To highlight this similarity, we plot the spectrum of Cyg X-1 from a 21 ks *RXTE* exposure taken on 1996 October 23 in each of the panels in Figure 2. Both the black holes and the neutron stars are dominated by Comptonized spectra of $kT \sim 100$ keV and $\tau \lesssim 1$, plus a cool $kT \lesssim 1$ keV soft excess and reflection from an optically thick accretion disk. The spectra of the black hole candidates, however, are often a bit flatter ($\Gamma \approx 1.5$) than the neutron star systems ($\Gamma \approx 2$).

2.1.2. X-ray Timing

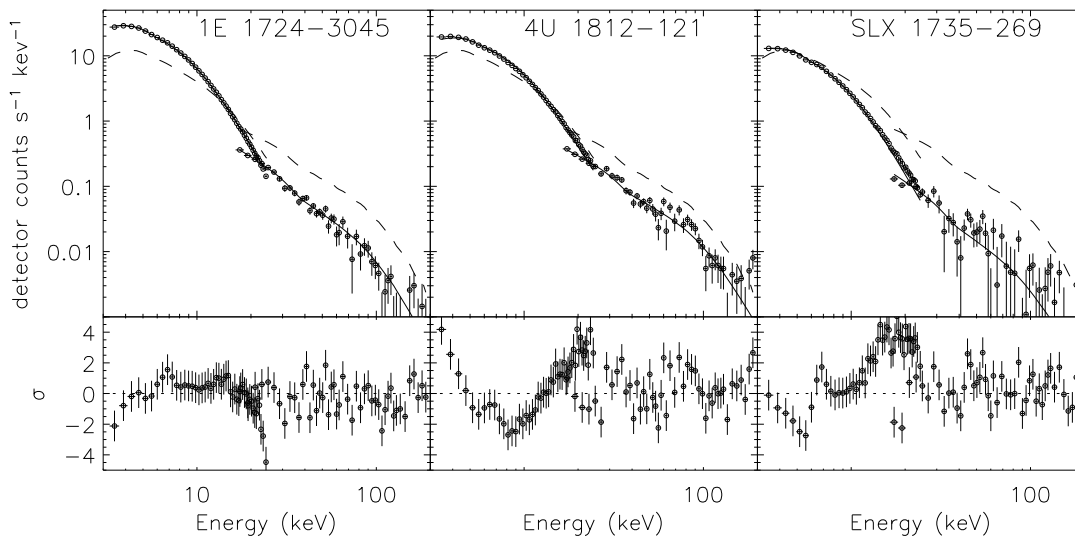


FIG. 2.— PCA and HEXTE spectra of the sources in this study, in units of detector counts. The residuals from the best-fit absorbed Comptonization spectra are displayed in the bottom panels, in units of the uncertainty in the data. Residuals between 6–20 keV in 4U 1812–12 and SLX 1735–269 are probably produced by hard photons that reflect off the optically thick accretion disk. We have plotted the spectrum of Cyg X-1 in the hard state with a dashed line, for comparison to this sample of neutron star LMXBs.

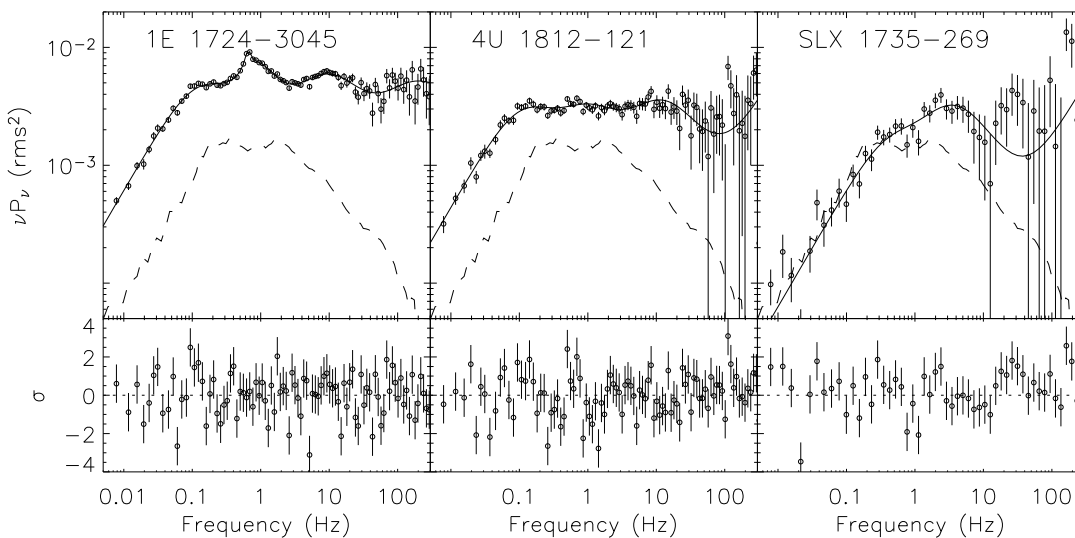


FIG. 3.— Power spectra of the neutron star LMXBs. The *bottom panels* illustrate the residuals to the fit of several Lorentzians to the data. The power spectrum of Cyg X-1 in the hard state is illustrated with the dashed line, which has been scaled downward by a factor of 10 for clarity. The timing data from the neutron star LMXBs have more power above 20 Hz, but are otherwise very similar to that of Cyg X-1.

We produced power spectra using PCA data with 122 μs (2^{-13} s) time resolution in a single energy channel (effectively 2–30 keV). We computed power spectra in 256 s intervals, and averaged them weighted by the total counts to produce an accurate estimate of the continuum power. We then subtracted the deadtime-corrected Poisson noise level from the power spectra (Zhang et al. 1996), re-binned them logarithmically, and estimated uncertainties from the standard deviation in the individual points averaged to compute the final power spectrum.

To quantify the shape of the power spectrum, we modeled the continuum with several zero-centered Lorentzian functions, and any QPOs with Lorentzians with variable centroid frequencies. We added Lorentzians until doing so no longer led to a significant decrease in χ^2 . The results are listed in Table 4, and displayed in Figure 3.

As before, the power spectra of these LMXBs strongly resemble those from black hole candidates such as Cyg X-1 and GX 339-4 in the hard state (Nowak et al. 1999; Smith & Liang 1999; Nowak 2000). For reference, we

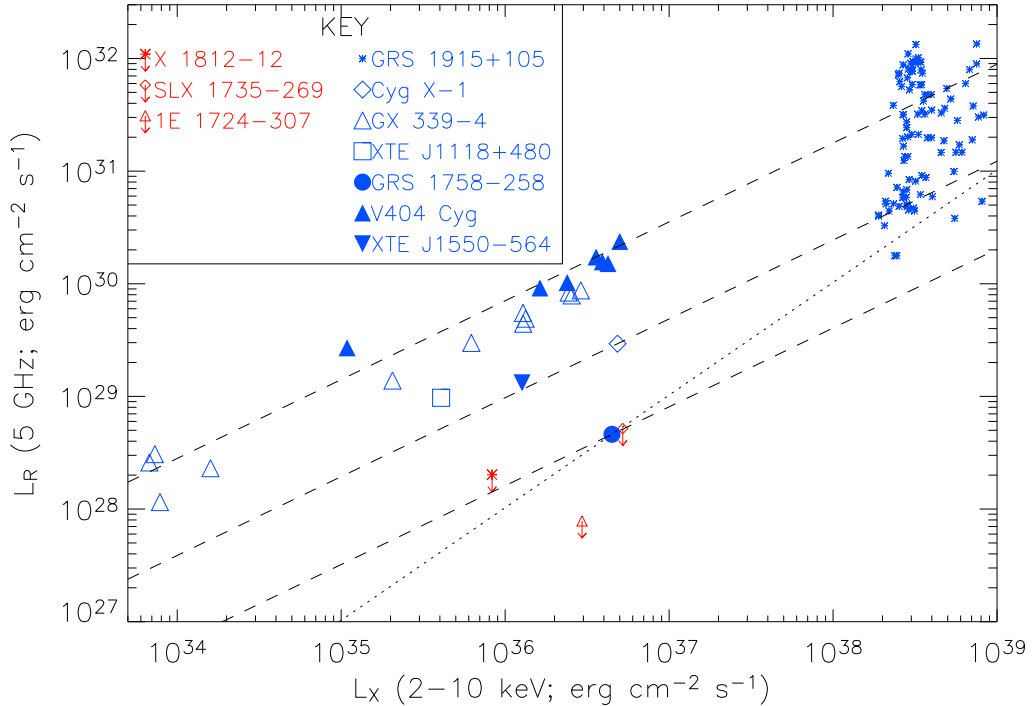


FIG. 4.— Comparison of the radio and X-ray luminosity of the neutron star LMXBs in our sample (red symbols), with those from several black hole candidates in the hard X-ray state (blue symbols). The *dashed lines* represent the observed $L_R \propto L_X^{0.7}$ correlations observed for several individual sources. The *dotted line* illustrates a linear $L_R \propto L_X$ proportionality that is normalized to the radio flux from GRS 1758–258. The radio flux is defined as that in a 5 GHz band around a central frequency of 5 GHz, assuming a flat radio spectrum. If 5 GHz measurements were not available, then either measurements at other frequencies were interpolated onto 5 GHz, or measurements at a single frequency were used under the assumption that the spectrum was flat (this introduced at most a 10% error). The X-ray luminosity is defined as that between 2–10 keV, deabsorbed. Values taken in different energy bands were extrapolated into the 2–10 keV band using the observed spectrum, or in one case (V404 Cyg) assuming a $\Gamma = 1.5$ power law spectrum. Distances to the neutron star systems were obtained as follows: for 1E 1724–307, we used the distance to Terzan 2 (4.1 kpc; Barbury, Bica, & Ortolani 1998); for 4U 1812–12, we used the peak flux of an Eddington-limited burst (6.6 kpc, taking $L_{\text{Edd}} = 3.5 \times 10^{38}$ erg s $^{-1}$ for pure He; Murakami et al. 1983); for SLX 1735–269, we assumed that a burst that had no spectral information was Eddington-limited and derived an upper limit to the distance (< 12 kpc; Bazzano et al. 1997). For the black hole candidates, the distances were taken from McClintock & Remillard (2004), except for GRS 1758–258, which was taken from Gallo et al. (2003). References for radio and X-ray fluxes of the black hole systems are as follows: GRS 1915+105 (Muno et al. 2001), Cyg X-1 (Stirling et al. 2001; Di Salvo et al. 2001), GX 339–4 (Corbel et al. 2003), XTE J1118+480 (McClintock et al. 2001; Fender et al. 2001), V404 Cyg (Han & Hjellming 1992), XTE J1550–564 (Corbel et al. 2001; Tomsick, Corbel, & Kaaret 2001), GRS 1758–258 (Lin et al. 2000).

have displayed the power spectrum of Cyg X-1 from 1996 October 23 in each panel of Figure 3. As noted by Sunyaev & Revnivtsev (2000) and Belloni et al. (2002), the main difference is that the neutron star systems exhibit more power continuum above 20 Hz.

2.2. VLA

The VLA is a multi-frequency, multi-configuration aperture synthesis imaging instrument, consisting of 27 antennas of 25 m diameter. We obtained VLA observations of 4U 1812–12 under program AR 458, and of 1E 1724–307 and SLX 1735–269 under program AM 703 (Table 1). The observation under AR 458 was a 15 minute integration at 8.45 GHz. The observations under program AM 703 were 1 hour integrations at 1.42 GHz and 2 hour integrations at 5.0 and 8.45 GHz. In all cases, we obtained 2 adjacent bands of 50 MHz nominal bandwidth processed in continuum mode. Calibration and imaging were carried out with standard tasks in the NRAO Astronomical Image Processing System (AIPS) package.

None of the three sources were detected in the radio.

We estimated 1- σ upper limits to the radio flux by measuring the rms dispersion in the noise within 5'' of each source. These upper limits are listed in Table 1.

3. DISCUSSION

We have placed the first strict upper limits on the radio emission from neutron star LMXBs that are known to have been in hard X-ray states. In Figure 4, we compare the luminosities of these neutron star LMXBs in the radio and X-ray bands with those of several black hole X-ray binaries. For the black holes, the luminosities were obtained from the references tabulated by Gallo et al. (2003, see the figure caption for details), using the most current distances listed in McClintock & Remillard (2004). The neutron star LMXBs in our sample have the lowest radio luminosities of the X-ray binaries in Figure 4.

Several authors have found that the relationship between the X-ray and radio luminosities of both individual black hole systems and the ensemble of systems follows the relationship $L_R \propto L_X^{0.7}$

(Corbel et al. 2003; Gallo et al. 2003). Remarkably, this scaling follows the spectral energy distribution expected from models of a standard conical radio jet that extracts a fixed fraction of the total

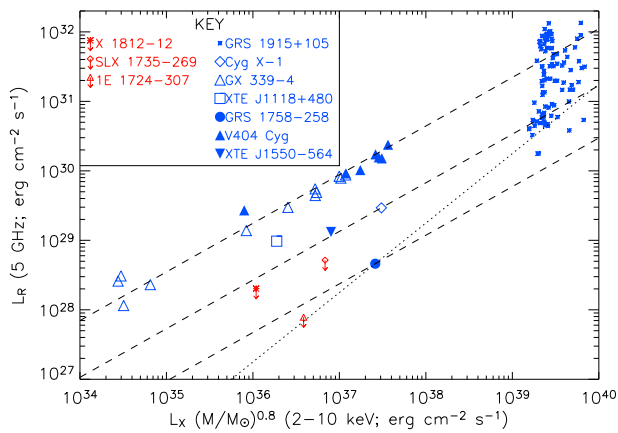


FIG. 5.— Same as Figure 4, except that the X-ray luminosity includes an extra mass-dependent term $(M/M_{\odot})^{0.8}$. Including this mass-dependence demonstrates that the radio upper limits from the three neutron star systems are all consistent with the fundamental plane defined by the faintest black hole system, GRS 1758–258.

energy from accretion (Blandford & Konigl 1979; Markoff et al. 2003; Heinz & Sunyaev 2003, Merloni, Heinz, & di Matteo 2003). Therefore, we also plot in Figure 4 lines of $L_R \propto L_X^{0.7}$ that intercept data from V404 Cyg, Cyg X-1, and GRS 1758–258; these lines bound the observed scatter in radio luminosities. The upper limits on the radio luminosities of the neutron star X-ray binaries are equal to or below the line of $L_R \propto L_X^{0.7}$ that passes through the faintest black hole X-ray binary observed in the hard X-ray state, GRS 1758–258 (Lin et al. 2000; Martí et al. 2002). The strictest 1- σ upper limit on the radio luminosity, from 1E 1724–307, is a factor of ≈ 4 below the relationship for GRS 1758–258. For comparison, there is a factor of ≈ 30 difference in the radio luminosities of GRS 1758–258 and those of V404 Cyg and GX 339–4.

By comparing a sample of accreting black holes in X-ray binaries and active galactic nuclei, Merloni et al. (2003) and (Falke et al. 2004) have found an additional dependence on black hole mass: $\log L_r = 0.6 \log L_X + 0.8 \log M$. This dependence is also expected from conical jet models (Falke et al. 2004; Robertson & Leiter 2004). Therefore, in Figure 5 we re-plot the data in Figure 4 with the x -axis scaled by a factor $(M/M_{\odot})^{0.8}$. Since all of the black holes in the sample have masses that are between 5–15 M_{\odot} (McClintock & Remillard 2004), the proposed dependence on mass does not account for the scatter in the L_R vs. L_X relationship for black holes. However, accounting for the fact that the neutron stars are likely to have masses near 1.4 M_{\odot} (Thorsett & Chakrabarty 1999) shifts them so that the upper limits on their radio luminosities are consistent with the relationship defined by GRS 1758–258. However, the mean luminosity of the neutron star LMXBs is still lower than that of the black holes.

Unfortunately, the individual upper limits on the radio emission from the three neutron star LMXBs are not

strict enough to establish a clear difference between the production of jets from accreting black holes and neutron stars. Nevertheless, the low radio luminosities of the neutron star systems do raise further questions as to the origin of the dispersion in the radio luminosities of accreting X-ray binaries in hard X-ray states. Gallo et al. (2003) suggested that GRS 1758–258 has an anomalously low radio luminosity because its jets have been “quenched” by an unknown mechanism that begins to operate when black holes accrete at a few percent of the Eddington rate. Indeed, all four sources with low radio luminosities have $L_X \approx (0.01 - 0.04)L_{\text{Edd}}$. However, the quenching mechanism would have to activate in these systems without manifesting any obvious cause (or reaction) in the energy spectrum and timing properties of the X-ray emission (see Lin et al. 2000 for GRS 1758–258, and Figures 2 and 3 for the neutron star LMXBs).

Further insight into the possible causes of the relative faintness of the radio emission during the hard X-ray states of GRS 1758–258, 1E 1724–307, 4U 1812–12, and SLX 1735–269 can be found by considering current models explaining why hard X-ray and radio emission are observed together. For instance, several authors have suggested that the structure of the accretion flow is more conducive to launching jets in the hard state than in the soft, most likely because the geometry of the accretion flow differs (Meier, Koide, & Uchida 2001; Meier 2001; Merloni & Fabian 2002). Specifically, the hard X-ray state is thought to occur when the accretion flow is radiatively inefficient and geometrically thick, whereas the thermal-dominated state is assumed to occur when the accretion disk is radiatively-efficient and geometrically thin (e.g., Esin, McClintock, & Narayan 1997). At the same time, the jets are assumed to be formed by threading matter onto a poloidal magnetic field anchored to the rotating accretion flow (Blandford & Payne 1982), while the fields are generated by turbulent motions in the accretion flow. Since the scale heights of the turbulent motions are much larger when the flow is geometrically thick, stronger magnetic fields and more powerful jets are produced in the hard state. Under this model, there is no obvious reason to associate the faintness of the radio emission from GRS 1758–258 and the neutron star LMXBs with the “quenching” of what would otherwise be a powerful compact jet, since the X-ray emission from these sources are almost indistinguishable from those of radio-luminous sources such as Cyg X-1. Instead, it seems more natural to assume that another physical or observational property of the radio-faint sources differs from the radio-luminous ones.

Another basic explanation for the association is that the hard X-rays are produced by optically-thin synchrotron emission from the electrons in the jet (Markoff, Falcke, & Fender 2001; Markoff et al. 2003; note that in this case the mechanism for launching the jet is unspecified). Under this model, there is little freedom to assume that the jet power is simply lower in GRS 1758–258 and the neutron star LMXBs during their hard states, because the X-ray emission is produced in the jet. One option is to assume that the break frequency at which the synchrotron emission from the jet changes from optically thick to optically thin shifts to higher frequencies, so that the X-ray luminosity from the jet is preserved, while the radio luminosity at 5 GHz declines.

This could be accommodated if the shock that accelerates the X-ray emitting electrons in the jet forms closer to the accreting compact object. Since the shock is positioned $\sim 10^3$ gravitational radii from the black holes in the models for XTE J1118+480 and GX 339-4 presented by Markoff et al. (2001, 2003), in principle there is plenty of room for it to move. Moreover, the presence of stronger noise in the power spectra of the neutron star LMXBs above ~ 20 Hz in Figure 3 could also be taken as evidence that the X-ray emitting region is closer to the compact object.⁸ Alternatively, some of the X-ray emission may be produced by synchrotron self-Compton emission, which would allow for some decoupling between the X-ray and radio emission (S. Markoff, M. Nowak, & J. Wilms, in preparation).

Given the tentativeness of the above arguments, we believe it also is important to consider whether the dispersion observed in the radio luminosity from the ensemble of black hole and neutron star X-ray binaries is caused by differences in the physical or observational parameters of the systems. For instance, Gallo et al. (2003) examined the degree to which Doppler boosting of the radio and X-ray emission could produce dispersion in the L_R vs. L_X relationship, and concluded that the tightness of the correlation between 10^{34} and $10^{36.5}$ erg s⁻¹ implies that the bulk motion of the jets can be no more than $\sim 0.8c$. However, they specifically omitted the data from GRS 1758-258, which they assumed was quenched in the radio; including that source and the neutron star LMXBs could point toward a larger importance for Doppler boosting.

The presence of a hard surface near the inner edge of the accretion disk is another factor that distinguishes neutron star LMXBs from those containing black holes. The hard surface must arrest the accretion flow, which would form a boundary layer (e.g., Popham & Sunyaev 2001) that could alter the structure of a jet or produce photons that cool the electrons in the jet. However, it is difficult to believe that this is the explanation for the faintness of the radio emission from the neutron stars, because there are not significant differences in the X-ray spectral or timing components seen from the black hole and neutron star systems that can be attributed unambiguously to such a boundary layer in the latter systems (Fig. 2 and 3).

Finally, it has also been suggested that the depth of the gravitational potential out of which the jets are produced can greatly influence their strength (e.g., Blandford & Payne 1982; Wilson & Colbert 1995; Meier 2001). In black hole systems, the inner radius at which a stable accretion disk can exist depends on the black hole spin; in a neutron star systems, it is most likely set by either the surface of the star, or by a dipole field anchored to the star. The low radio luminosities of GRS 1758-298, 1E 1724-307, 4U 1812-12, and SLX 1735-269 could then be explained by the relative shallowness of their potentials. For the neutron stars, the difference would be due

to the nature of the compact object; for GRS 1758-258, the difference could be explained if the black hole was either non-rotating, or rotating with an angular momentum opposite to that of the accretion disk.

4. CONCLUSIONS

We have obtained upper limits on the radio emission from three neutron star LMXBs, concurrent with X-ray observations that demonstrated that they were in a hard X-ray state. We have compared these upper limits to the radio luminosities of several black holes in very similar hard states, and found that the neutron star systems are as faint as or fainter than the black hole candidate with the lowest observed radio luminosity, GRS 1758-258. The difference in radio luminosity can partly be attributed to the lower masses of the neutron star systems, which on theoretical and observational grounds is expected to decrease as $M^{0.8}$. However, there still remains a factor of 30 scatter in the radio luminosities of black hole and neutron star X-ray binaries, particularly at X-ray luminosities of a few percent Eddington. We find no obvious differences in the X-ray timing and spectral properties that explain this dispersion.

Two future observations could help resolve why there is such a large dispersion in the radio luminosities of black hole X-ray binaries, and why neutron stars tend to fall on or below the faint end of this dispersion. First, it is important to either detect, or place much stricter upper limits on, the radio luminosities of neutron star LMXBs in the X-ray hard state. This would help resolve whether there is indeed a physical difference that causes the relative faintness of neutron star LMXBs, or whether the three sources we observe just happen to fall on the low end of a dispersion in radio luminosity. Second, radio observations of the fainter radio sources, i.e. GRS 1758-298 and the neutron star LMXBs, at lower X-ray luminosities could reveal whether they are indeed quenched near $L_{\text{Edd}} \sim 0.01$, or whether another parameter is needed to explain the radio luminosity of X-ray binaries in hard states.

We are grateful to the VLA and *RXTE* planning teams, particularly B. Clark and E. Smith, for coordinating these observations. We also thank S. Markoff and R. Fender for helpful conversations and encouragement while pursuing this work. This research has made use of data obtained through the High Energy Astrophysics Science Archive Research Center, provided by NASA through the Goddard Space Flight Center. M. Munro was supported through a Hubble Fellowship grant (program number HST-HF-01164.01-A) from the Space Telescope Science Institute, which is operated by the Association of Universities for Research in Astronomy, Incorporated, Under NASA contract NAS5-26555.

and GX 339-4.

REFERENCES

Bachiller, R. 1996, *ARA&A*, 34, 111
 Barret, D. et al. 1991, *ApJ*, 379, L21

Barret, D., Grindlay, J. E., Harrus, I. M., & Olive, J. F. 1999, *A&A*, 341

⁸ It has not been reported in the literature whether high frequency noise is stronger in GRS 1758-258 than in, e.g., Cyg X-1

- Barret, D., Olive, J. F., Boirin, L., Done, C., Skinner, G. K., & Grindlay, J. E. 2000, *ApJ*, 533, 329
- Barret, D., Olive, J. F., & Oosterbroek, T. 2003, *A&A*, 400, 643
- Bazzano, A., Cocchi, M., Ubertini, P., Heise, J., in 't Zand, J., & Muller, J. M. 1997, *IAU Circ.*, 6668
- Belloni, T., Klein-Wolt, M., Méndez, M., van der Klis, M., & van Paradijs, J. 2000, *A&A*, 355, 271
- Belloni, T., Psaltis, D., & van der Klis, M. 2002, *ApJ*, 572, 392
- Berendsen, S. G. H., Fender, R., Kuulkers, E., Heise, J., & van der Klis 2000, *MNRAS*, 318, 599
- Blandford, R. D. & Konigl, A. 1979, *ApJ*, 232, 34
- Blandford, R. D. & Payne, D. G. 1982, *MNRAS*, 199, 883
- Brocksopp, C., Fender, R. P., Larionov, V., Lyuty, V. M., Tarasov, A. E., Pooley, G. G., Paciasas, W. S., & Roche, P. 1999, *MNRAS*, 309, 1063
- Corbel, S., Fender, R. P., Tzioumis, A. K., Nowak, M., McIntyre, V., Durouchoux, P., & Sood, R. 2000, *A&A*, 359, 251
- Corbel, S., Kaaret, P., Jain, R. K., Bailyn, C. D., Fender, R. P., Tomsick, J. A., Kalemci, E., McIntyre, V., Campbell-Wilson, D., Miller, J. M. & McCollough, M. L. 2001, *ApJ*, 554, 43
- Corbel, S., Nowak, M. A., Fender, R. P., Tzioumis, A. Z., & Markoff, S. 2003, *A&A*, 400, 1007
- Cowley, A. P., Schmidtke, P. C., Crampton, D., & Hutchings, J. B. 1998, *ApJ*, 504, 854
- Crocker, M. M., Davis, R. J., Spencer, R. E., Eyres, S. P. S., Bode, M. F., & Skopal, A. 2002, *MNRAS*, 335, 1100
- David, P., Goldwurm, A., Murakami, T., Paul, J., Laurent, P., & Goldoni, P. 1997, *A&A*, 322, 229
- Dhawan, V., Mirabel, I. F., & Rodríguez, L. F. 2000, *ApJ*, 543, 373
- Di Salvo, T., Done, C., Zycki, P. T., Burderi, L., & Robba, N. R. 2001, *ApJ*, 547, 1024
- Done, C. & Gierliński, M. 2003, *MNRAS*, 342, 1041
- Esin, A. A., McClintock, J. E., & Narayan, R. 1997, *ApJ*, 489, 865
- Fabian, A. C., Rees, M. J., Stella, L., & White, N. E. 1989, *MNRAS*, 238, 729
- Falcke, H., Körding, E., & Markoff, S. 2004, *A&A*, 414, 895
- Fender, R. P. 2004, to appear in "Compact Stellar X-ray Sources", eds. W. H. G. Lewin & M. van der Klis, Cambridge University Press, astro-ph/0303339
- Fender, R., Wu, K., Johnston, H., Tzioumis, T., Jonker, P., Spencer, R., & van der Klis, M. 2004a, *Nature*, 427, 222
- Fender, R. P., Belloni, T. M., & Gallo, E. 2004b, *MNRAS* in press, astro-ph/0409360
- Fender, R. P. & Kuulkers, E. 2001, *MNRAS*, 324, 923
- Fender, R. P., Garrington, S. T., McKay, D. J., Muxlow, T. W. B., Pooley, G. G., Spencer, R. E., Stirling, A. M., & Waltman, E. B. 1999, *MNRAS*, 304, 865
- Fender, R. P., Hjellming, R. M., Tilanus, R. P. J., Pooley, G. G., Deane, J. R., Ogley, R. N., & Spencer, R. E. 2001, *MNRAS*, 322, L23
- Fomalont, E. B., Geldzahler, B. J., & Bradshaw, C. F. 2001, *ApJ*, 553, L27
- Gallo, E., Fender, R. P., & Pooley, G. G. 2003, *MNRAS*, 344, 60
- Grindlay, J. E., Marshall, H. L., Hertz, P., Soltan, A., Weisskopf, M. C., Elsner, R. F., Ghosh, P., Darbro, W., & Sutherland, P. G. 1980, *ApJ*, 240, L121
- Guainazzi, M., Parmar, A. N., Segreto, A., Stella, L., Dal Fiume, D., & Oosterbroek, T. 1998, *A&A*, 339, 802
- Han, X. & Hjellming, R. M. 1992, *ApJ*, 400, 304
- Hartmann, L. & Kenyon, S. J. 1996, *ARA&A*, 34, 207
- Heinz, S. & Sunyaev, R. A. 2003, *MNRAS*, 343, L59
- Homan, J., Wijnands, R., Rupen, M. P., Fender, R., Hjellming, R. M., di Salvo, T., & van der Klis, M. 2003, astro-ph/0309042
- Jahoda, K., Swank, J. H., Giles, A. B., Stark, M. J., Strohmayer, T., Zhang, W., & Morgan, E. H. 1996, in *Proc. SPIE 2808, EUV, X-Ray, and Gamma-Ray Instrumentation for Astronomy VII*, ed. O. H. Siegmund & M. A. Gummin (Bellingham: SPIE), 59
- Keck, J. W. et al. 2001, *ApJ*, 563, 301
- Levine, A. M., Bradt, H., Cui, W., Jernigan, J. G., Morgan, E. H., Remillard, R., Shirey, R. E., & Smith, D. A. 1996, *ApJ*, 469, L33
- Lin, D., Smith, I. A., Liang, E. P., Bridgman, T., Smith, D. M., Martí, J., Durouchoux, Ph., Mirabel, I. F., & Rodríguez, L. F. 2000, *ApJ*, 532, 548
- Lynden-Bell, D. 1996, *MNRAS*, 279, 389
- Magdziarz, P. & Zdziarski, A. A. 1995, *MNRAS*, 273, 837
- Markoff, S., Falcke, H., & Fender, R. 2001, *A&A*, 372, L25
- Markoff, S., Nowak, M., Corbel, S., Fender, R., & Falcke, H. 2003, *A&A*, 397, 645
- Martí, J., Mirabel, I. F., Rodríguez, L. F., & Smith, I. A. 2002, *A&A*, 386, 571
- McClintock, J. E. et al. 2001, *ApJ*, 555, 477
- McClintock, J. E. & Remillard, R. A. 2004, to appear in "Compact Stellar X-ray Sources", eds. W. H. G. Lewin & M. van der Klis, Cambridge University Press, astro-ph/0306213
- Meier, D. L. 2001, *ApJ*, 2001, 548, L9
- Meier, D. L., Koide, S., & Uchida, Y. 2001, *Science*, 291, 84
- Merloni, A., Heinz, S., & di Matteo, T. 2003, *MNRAS*, 345, 1057
- Merloni, A. & Fabian, A. C. 2002, *MNRAS*, 332, 165
- Migliari, S., Fender, R. P., Rupen, M., Jonker, P. G., Klein-Wolt, M., Hjellming, R. M., & van der Klis, M. 2003, *MNRAS*, 342, L67
- Migliari, S., Fender, R. P., Rupen, M., Wachter, S., Jonker, P. G., Homan, J. & van der Klis, M. 2004, astro-ph/0402600
- Mirabel, I. F. & Rodríguez, L. F. 1994, *Nature*, 371, 46
- Mirabel, I. F., Dhawan, V., Chaty, S., Rodríguez, L. F., Martí, J., Robinson, C. R., Swank, J., Geballe, T. 1998, *A&A*, 300, L9
- Muno, M. P., Remillard, R. A., & Chakrabarty, D. 2002, *ApJ*, 568, L35
- Muno, M. P., Remillard, R. A., Morgan, E. H., Waltman, E. B., Dhawan, V., Hjellming, R. M., & Pooley, G. 2001, *ApJ*, 556, 515
- Murakami, T. et al. 1983, *PASJ*, 35, 531
- Nowak, M. A. 2000, *MNRAS*, 318, 361
- Nowak, M. A., Vaughan, B. A., Wilms, J., Dove, J. B., & Begelman, M. C. 1999, *ApJ*, 510, 874
- Olive, J. F., Barret, D., Boirin, J., Grindlay, J. E., Swank, J. H., & Smale, A. P. 1998, *A&A*, 333, 942
- Penninx, W., Lewin, W. H. G., Zijlstra, A. A., Mitsuda, K., & van Paradijs, J. 1988, *Nature*, 336, 146
- Popham, R. & Sunyaev, R. 2001, *ApJ*, 547, 355
- Revnivtsev, M. G., Trudolyubov, S. P., & Borozdin, K. N. 2002, *Astronomy Letters*, 28, 237
- Robertson, S. L. & Leiter, D. J. 2004, astro-ph/0402445
- Rothschild et al. 1998, *ApJ*, 496, 538
- Shakura, N. I. & Sunyaev, R. A. 1973, *A&A*, 24, 337
- Smith, I. A. & Liang, E. P. 1999, *ApJ*, 519, 771
- Sokoloski, J. L. & Kenyon, S. J. 2003, *ApJ*, 584, 1021
- Stirling, A. M., Spencer, R. E., de la Force, C. J., Garret, M. A., Fender, R. P., & Ogley, R. N. 2001, *MNRAS*, 327, 1273
- Sunyaev, R. & Revnivtsev, M. 2000 *A&A*, 358, 617
- Tavani, M., Fruchter, A., Zhang, S. N., Harmon, B. A., Hjellming, R. N., Rupen, M. P., Bailyn, C., & Livio, M. 1996, *ApJ*, 473, L103
- Thorsett, S. E. & Chakrabarty, D. 1999, *ApJ*, 512, 288
- Titarchuk, L. 1994, *ApJ*, 434, 313
- Tomsick, J. A., Corbel, S., & Kaaret, P. 2001, *ApJ*, 563, 229
- van der Klis, M. 1995, in *X-Ray Binaries*, ed. W. H. G. Lewin, J. van Paradijs, & E. P. J. van den Heuvel (Cambridge U. Press), 252
- Wijnands, R. & van der Klis, M. 1999, *A&A*, 345, L35
- Wilms, J., Nowak, M. A., Dove, J. B., Fender, R. P., & Di Matteo, T. 1999, *ApJ*, 522, 460
- Wilson, A. S. & Colbert, E. J. M. 1995, *ApJ*, 438, 62
- Wilson, C., Patel, S. K., Kouveliotou, C., Jonker, P. G., van der Klis, M., Lewin, W. H. G., Belloni, T., & Méndez, M. 2003, *ApJ*, 596, 1220
- Zhang, W., Morgan, E. H., Jahoda, K., Swank, J. H., Strohmayer, T. E., Jernigan, G., & Klein, R. I. 1996, *ApJ*469, L29

TABLE 1
VLA OBSERVATIONS

| Source | RA (J2000) | DEC | Date | ν (GHz) | T_{Exp} (h) | S_ν (mJy) |
|--------------|---------------|-------------|-------------|----------------|-------------------------|------------------|
| 4U 1812–12 | 18 15 06.18 | –12 05 47.1 | 2001 Jun 5 | 8.4 | 0.25 | < 0.2 |
| SLX 1735–269 | 17 38 17.12 | –26 59 38.6 | 2001 Nov 5 | 8.4 | 1.5 | < 0.056 |
| | | | | 1.5 | 1.5 | < 0.16 |
| 1E 1724–307 | 17 27 33.15 | –30 48 07.8 | 2001 Sep 25 | 8.4 | 1 | < 0.025 |
| | | | | 4.8 | 1 | < 0.035 |
| | | | | 1.4 | 1 | < 0.41 |

NOTE. — Positions were taken from Revnivtsev, Trudolyubov, & Borozdin (2002) and Wilson et al. (2003).

TABLE 2
RXTE OBSERVATIONS

| Source | Date | T_{Exp} (ks) | No. PCU | C (c s ^{–1} PCU ^{–1}) | HC |
|--------------|-------------------------|--------------------------|---------|---|-------|
| 4U 1812–12 | 2001 Jun 6 – Jul 21 | 21 | 3.0 | 41 | 0.824 |
| SLX 1735–269 | 2001 Nov 5 – 7 | 22 | 2.8 | 31 | 0.693 |
| 1E 1724–307 | 2001 Sep 25; Nov 9 – 11 | 48 | 3.3 | 54 | 0.706 |

NOTE. — For each source, we list the date of the PCA observations, the exposure time, the average number of active proportional counter units, the count rate, and the hard color.

TABLE 3
X-RAY SPECTRA

| Parameter | 4U 1812–12 | SLX 1735–269 | 1E 1724–307 |
|--|--|--|---|
| N_{H} (cm ^{–2} ; fixed) | 1.5 | 1.5 | 1.0 |
| kT_{bb} (keV) | 0.59 ^{+0.03} _{–0.04} | 0.48 ^{+0.03} _{–0.12} | ... |
| N_{bb} (km [10 kpc] ^{–1}) | 73 ⁺¹⁶ _{–19} | 150 ⁺¹¹⁵⁰ _{–70} | ... |
| Γ | 1.70 ^{+0.03} _{–0.05} | 2.00 ^{+0.03} _{–0.03} | 1.96 ^{+0.02} _{–0.0} |
| E_{fold} (fixed) | 300 | 300 | 300 |
| R | 0.27 ^{+0.07} _{–0.02} | 0.45 ^{+0.05} _{–0.09} | < 0.003 |
| ξ (erg cm s ^{–1}) | 0.25 | 654 | ... |
| N_{Γ} (ph cm ^{–2} s ^{–1}) | 0.10 ^{+0.05} _{–0.02} | 0.11 ^{+0.01} _{–0.01} | 0.207 ^{+0.001} _{–0.001} |
| χ^2/ν | 92/87 | 78/88 | 106/90 |
| $F_{2-10\text{keV}}$ (10 ^{–10} erg cm ^{–2} s ^{–1}) | 4.1 | 3.0 | 5.6 |
| $F_{10-20\text{keV}}$ (10 ^{–10} erg cm ^{–2} s ^{–1}) | 2.5 | 1.8 | 2.4 |
| $F_{20-200\text{keV}}$ (10 ^{–10} erg cm ^{–2} s ^{–1}) | 6.8 | 1.9 | 4.9 |

NOTE. — All fluxes are de-absorbed.

TABLE 4
X-RAY TIMING

| Parameter | 4U 1812–12 | SLX 1735–269 | 1E 1724–307 |
|-------------------------------|------------------------------------|---|------------------------------------|
| constant ($\times 10^{-6}$) | 11(4) | 4(1) | 16(5) |
| ν_1, W_1, N_1 | 0, 0.25(3), 0.039(3) | 0, 0.28(1), 0.056(5) | 0, 0.9(2), 4.7(6) $\times 10^{-3}$ |
| ν_2, W_2, N_2 | < 0.5, 2(1), 2(1) $\times 10^{-3}$ | 0, 3.0, 2.0(9) $\times 10^{-3}$ | 0, 7(1), 1.5(4) $\times 10^{-3}$ |
| ν_3, W_3, N_3 | 0, 25(6), 5(2) $\times 10^{-4}$ | 0, 19.3(9), 1.0(1) $\times 10^{-3}$ | ... |
| ν_4, W_4, N_4 | ... | 0, 371(90), 4.2(7) $\times 10^{-5}$ | ... |
| ν_5, W_5, N_5 | ... | 0.64(1), 0.17(7), 4.4(5) $\times 10^{-3}$ | ... |
| ν_6, W_6, N_6 | ... | 0.62(8), 1.4(2), 6(1) $\times 10^{-3}$ | ... |
| χ^2/ν | 135/98 | 119/89 | 76/54 |

NOTE. — Power spectra were fit with Lorentzians, the parameters of which were the centroid (ν_i), width (W_i) and normalization (N_i).